Mechanical and electronic properties of ferromagnetic $Ga_{1-x}Mn_xAs$ using ultrafast coherent acoustic phonons

J. Qi (齐静波),[1] J. A. Yan (严家安),[1] H. Park,[1] A. Steigerwald,[1] Y. Xu (徐滢),[1] S. N. Gilbert,[1] X. Liu,[2] J. K. Furdyna,[2] S. T. Pantelides,[1] and N. Tolk[1]

[1]*Department of Physics and Astronomy, Vanderbilt University, Nashville, Tennessee 37235, USA*

[2]*Department of Physics, University of Notre Dame, Notre Dame, Indiana 46556, USA*

(Received 14 December 2009; revised manuscript received 7 February 2010; published 22 March 2010)

Ultrafast two-color pump-probe measurements, involving coherent acoustic phonon waves, have provided information simultaneously on the mechanical properties and on the electronic structure of ferromagnetic $Ga_{1-x}Mn_xAs$. The elastic constants C_{11} of $Ga_{1-x}Mn_xAs$ ($0.03 \leq x \leq 0.07$) are observed to be systematically smaller than those of GaAs. Both C_{11} and V_s measured in $Ga_{1-x}Mn_xAs$ are found to increase with temperature ($78\ \text{K} \leq T \leq 295\ \text{K}$), again in contrast to the opposite behavior in GaAs. In addition, our experimental results indicate a small blueshifting of the fundamental band gap of $Ga_{1-x}Mn_xAs$ as Mn concentration increases.

DOI: 10.1103/PhysRevB.81.115208 PACS number(s): 78.47.D−, 62.30.+d, 71.15.Mb, 62.20.−x

I. INTRODUCTION

The introduction of carrier-mediated III-Mn-V ferromagnetic semiconductors opens up promising opportunities to combine semiconducting properties and robust magnetism into conventional electrical and optical devices.[1,2] In the process of explaining recent experimental observations, along with attempts to develop a theory of hole-mediated ferromagnetism in "prototypical" ferromagnetic GaMnAs systems, the relationship between mechanical, magnetic, and electronic properties has been extensively explored.[2–4] For instance, much attention has been given to understanding of the effect of strain on the magnetic easy axis and on anisotropy fields arising from the substrate-film lattice mismatch.[5–8] Specifically, however, when constructing a theoretical model, due to the lack of corresponding experimental values for the GaMnAs system, values of elastic constants in the strain-associated Hamiltonian of GaMnAs are generally assumed to be the same as those of GaAs.[7–9] On the other hand, over the past several years the nature of the electronic structure in carrier-mediated ferromagnetism of $Ga_{1-x}Mn_xAs$ has been the subject of an important and lively debate.[2,3] One effective way to reveal the band structure of this material is to study the evolution of the critical points in energy by measuring relevant optical constants such as the complex refractive index $[\hat{n}=n+ik]$ or the complex dielectric constant $[\hat{\varepsilon}=\varepsilon_1+i\varepsilon_2]$.[3] Recently Burch *et al.*[10] used spectroscopic ellipsometry and observed a large blueshifting of the critical point E_1 with Mn doping. They attributed this to a Mn-induced impurity band (IB) existing in this material system and this IB has strongly hybridized with the GaAs valence band (VB) near the L point. However, they did not observe any changes for all other critical points as Mn concentration varies.

Although many time-domain studies of carrier and spin dynamics have been done on (III,Mn)V structures over the years, few experiments are reported to measure the mechanical properties and reveal the electronic structure of this system using pump-probe spectroscopy. In this paper, we report measurements of the elastic constant C_{11} utilizing an ultrafast pump-probe approach involving coherent acoustic phonons (CAPs) propagating in ferromagnetic $Ga_{1-x}Mn_xAs$ ($0.03 \leq x \leq 0.07$) systems. The measured values are found to be very different from those of GaAs and low-temperature grown GaAs (LT-GaAs). These observations are partially explained by density-functional calculations. Experimentally, we also observe a clear blueshift of the critical point E_0 (fundamental band gap) with Mn doping in $Ga_{1-x}Mn_xAs$.

II. SAMPLES AND EXPERIMENTAL SETUP

Our ferromagnetic $Ga_{1-x}Mn_xAs$ sample is grown by the low-temperature molecular-beam epitaxy method. Before the growth of the $Ga_{1-x}Mn_xAs$ ($x=0.03$, 0.05, and 0.07) layer with a thickness 1 μm, an LT-GaAs (~270 °C) buffer layer with a thickness 300 nm was grown on a semi-insulating GaAs(001) substrate. For the purpose of comparison, one GaAs(001) substrate and one LT-GaAs sample (with no Mn) with a layer thickness of 1.3 μm grown under similar conditions were also used in the experiment. The ferromagnetic $Ga_{1-x}Mn_xAs$ samples with $x=0.03$, 0.05, and 0.07 have Curie temperatures around 35, 55, and 53 K, respectively.

In our setup, we used a two-color all-optical pump-probe technique. The pump photon energies were around 3.1 eV (~400 nm), significantly above the fundamental band gap E_0 of GaAs [1.42 eV (~873 nm) at 295 K and 1.51 eV (~821 nm) at 78 K]. The probe light, on the other hand, is chosen to be near E_0. Such high pump photon energy leads to the creation of coherent phonons generated near the surface of the $Ga_{1-x}Mn_xAs$ layer arising from the femtosecond excitation light pulse. The subsequent CAP wave (strain pulse), which alters locally the optical properties (the complex refractive index), propagates into the $Ga_{1-x}Mn_xAs$/GaAs(001) and is detected by monitoring the reflected probe pulse. Such CAPs have been widely observed using pump-probe spectroscopic technique in many material systems.[11–16] All the following experiments measuring transient reflectivity changes $\Delta R/R$ were performed employing a Ti:Sapphire laser with a repetition rate of 76 MHz, which produces ~150 fs wide pulses in the wavelength range between ~720 and ~950 nm. The temperature can be varied between 78 and 295 K. Both pump and probe beams (typical intensity ratio

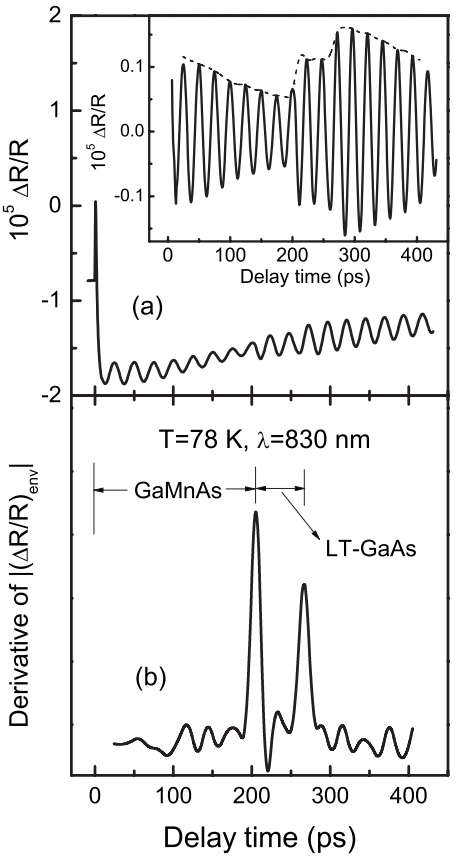

FIG. 1. (a) Pump-probe response of $Ga_{0.95}Mn_{0.05}As$/LT-GaAs/GaAs at 78 K for the probe wavelength 830 nm; (b) derivative of envelope of oscillations $|(\Delta R/R)_{env}|$ as a function of delay time. Inset: the subtracted oscillatory response and its envelope. The regimes determined by the GaMnAs and LT-GaAs layers are indicated by horizontal arrows in the inset, respectively.

of 8:1) were focused onto the sample at the same spot with a diameter of around 100 μm. The pump light typically had a fluence of 1 $\mu J/cm^2$.

III. RESULTS

Figure 1(a) shows the transient reflectivity signal $\Delta R/R$ measured in the $Ga_{0.95}Mn_{0.05}As$/GaAs sample at 78 K. The inset is the measured oscillatory response obtained by subtracting the relaxation background. The probe pulse is centered at 830 nm with photon energy somewhat below the fundamental band gap of GaAs (~821 nm). It can be seen that the total response consists of a fast transient (on the order of a few picoseconds) followed by a tail superimposed with two distinct damped oscillatory regimes, separated by a narrow transition region. The initial fast transient is typical of electronic contribution to the pump-probe signal.

The observed oscillations may be explained by a propagating strain pulse model,[11] where the oscillations originate from the interference of probe beams reflected from the top sample surface and the propagating strain pulse. The reflectivity change $\Delta R/R$ for the oscillatory behavior may be written[11]

$$\Delta R/R \propto Ae^{-t/\tau}\cos(2\pi t/T_p + \varphi), \quad (1)$$

where A is the amplitude, τ is the damping time, φ is phase shift, and T_p is the oscillation period given by $T_p = \lambda/(2nV_s \cos\theta)$. Here n is the refractive index, V_s is speed of sound, and θ (~0 in our experiments) is the angle of incidence of the probe light in GaMnAs with respect to the normal to sample surface. In the "near-field" approximation,[5] the damping time τ is further related to the absorption properties of the material by $\tau = 1/(2\alpha V_s) = \lambda(4\pi V_s\kappa)^{-1}$, where α is the absorption coefficient and κ is the imaginary part of the complex refractive index $\tilde{N}(=n+i\kappa)$. The amplitude A is, furthermore, connected to the change in the local complex refractive index through the z-component strain (η_{33}) by the relation $A \propto |\delta\tilde{N}/\delta\eta_{33}|$.[11,14]

The generated CAP wave first travels through $Ga_{1-x}Mn_xAs$ normal to the surface at the speed $V_{s(GaMnAs)}$ of the longitudinal acoustic phonon (LAP) before it reaches the LT-GaAs and GaAs regions. After passing through the $Ga_{1-x}Mn_xAs$/LT-GaAs interface, it continuously propagates into the LT-GaAs and GaAs layers with LAP speed $V_{s(LT\text{-}GaAs)}$ and $V_{s(GaAs)}$, respectively. We estimate that it takes about $\Delta t \approx 200$ ps for the strain pulse to arrive at the LT-GaAs layer assuming that $V_{s(GaMnAs)}$ is approximately equal to $V_{s(GaAs)}$ [$\sim 4.78\times 10^3$ m/s at 78 K (Ref. 17)]. This can be seen from the experimental results shown in Fig. 1.

We investigated the dependence of the oscillations near the band gap of GaAs on the probe wavelength. The oscillations induced by CAP waves traveling in the $Ga_{1-x}Mn_xAs$ layer decay markedly at all the wavelengths studied. In contrast, the oscillations in the GaAs response persist for a very long time at probe wavelengths below the band gap of GaAs. Applying Eq. (1) to the studied material, we can numerically fit our experimental data at different wavelengths, and obtain significant physical parameters, including the period, damping time, and amplitude of the oscillations. We note that the two-color pump-probe technique enables us to get the oscillation profiles with a high signal/noise ratio. Standard errors of parameters T_p and τ of the oscillation are less than 1% and 3%, respectively.

As is well known, the speed of LAP waves propagating along [001] is given by $V_s = (C_{11}/\rho)^{1/2}$ for cubic-symmetry solids with elastic constant C_{11} and density ρ. Therefore, using this equation and the expression $T_p = \lambda/(2nV_s)$, we can determine two of the important mechanical properties, the LAP speed V_s along [001] and the corresponding elastic constant C_{11}, which have never before been reported for the ferromagnetic $Ga_{1-x}Mn_xAs$ system. Here, we also report temperature (T) dependent measurements of C_{11}.

The refractive indices n of GaAs, LT-GaAs and $Ga_{1-x}Mn_xAs$ at room temperature (T=295 K) are directly measured by spectroscopic ellipsometry. In principle, the refractive index n depends on both temperature T and wavelength λ. In this study, at low temperatures we used n measured at T=295 K with shorter wavelengths (i.e., $\lambda \leq 800$ nm) above the fundamental band gap E_0 to obtain V_s. This means that we assume $n(T, \lambda \leq 800$ nm) is independent of T for 78 K $\leq T \leq$ 295 K. This assumption (or approximation) is based on two considerations:[18,19] (1) in the infrared

nonresonant absorption regime ($\lambda > 1$ μm), the refractive index and optical conductivity for both GaAs and GaMnAs change only very slightly as temperature varies between 78 and 295 K (~1% for GaAs) and (2) $n^{-1}dn/dT$ has relatively large values at the critical-energy points (i.e., E_0). However, the validity of this assumption needs to be carefully checked.

The calculated propagating time of the strain pulse inside different layers using the obtained V_s based on the above assumption and the known film thickness should be consistent with the value directly obtained from the oscillation amplitude in the reflectivity measurements. Our previous works[15,20] suggest that tracing the oscillation amplitude changes across different layers provides a very powerful tool in depth profiling and material characterizing of heterostructure semiconductors. The traveling time in different layers can be accurately acquired by taking the derivatives of the envelope of the oscillations. It should be pointed out that the instantaneous created strain pulse here has a spatial width of around 100 nm and is centered at ~50 nm away from the top surface, as determined by the absorption depth of pump light. Thus, e.g., at $T=78$ K for $Ga_{0.95}Mn_{0.05}As$ layer, according to the obtained value of $V_s=4655$ m/s and the effective propagating distance ~950 nm, the time can be estimated to be ~204 ps. The subsequent traveling time in 300-nm-thick LT-GaAs is ~62.9 ps with $V_s=4768$ m/s. These two values agree very well with ~205 ps for $Ga_{0.95}Mn_{0.05}As$ and ~62.5 ps for LT-GaAs derived from the oscillation profile without using index refraction n [see Fig. 1(b)]. Following the same procedure, we find that the relative change between the two methods is less than ~1% at different temperatures on different samples. Therefore, our assumption above is well supported by the experiments.

Moreover, we note that the obtained speed of sound V_s has to be independent of wavelength λ for $\lambda \leq 800$ nm. Our results between 78 and 295 K for 760 nm$\leq\lambda\leq$800 nm show that $|\Delta V_s|/V_s$ is less than 0.5%, which is quite small and confirms that V_s can be taken as constant. Therefore, reasonable V_s can be obtained at any wavelength between 760 and 800 nm. Here, the average value of V_s at two wavelengths (760 and 800 nm) is chosen and employed to calculate C_{11}.

In zinc-blende GaAs, thermal expansion has been measured to be very small in the temperature range of 50–300 K. The typical thermal-expansion-coefficient value is $\alpha_{th}=\frac{1}{a_0}\frac{da_0}{dT}=6\times10^{-6}$ K^{-1}.[18] For $Ga_{1-x}Mn_xAs$ ($x=0.01-0.09$), it is believed that the temperature dependence of lattice constants is almost the same as that in bulk GaAs, and the relaxed lattice constant for $Ga_{1-x}Mn_xAs$ follows the relation $a=0.566+(0.598-0.566)x$ nm.[1,2] Assuming the primary lattice location of Mn to be substitutional Mn_{Ga}, and up to ~20% of the Mn to reside in interstitial positions,[2] the density of the as-grown $Ga_{1-x}Mn_xAs$ sample is expected to be roughly the same as that of GaAs. In actual calculation of C_{11}, at 295 K, $\rho=5.317$ g/cm^3 was assumed for GaAs and LT-GaAs, and $\rho=5.317\times(1-0.169x)$ g/cm^3 was taken for $Ga_{1-x}Mn_xAs$. The thermal expansion was corrected in the same way using $\alpha_{th}=6\times10^{-6}$ K^{-1}. In fact, using a simple estimate based on the above value of α_{th}, the relative variation of C_{11} due to thermal expansion will not exceed 0.4%.

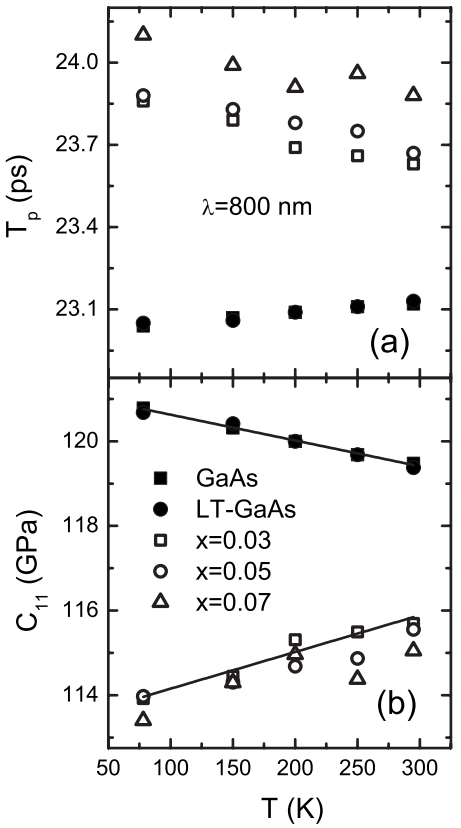

FIG. 2. (a) Oscillation period T_p at 800 nm and (b) elastic constant C_{11} as a function of temperature T for $Ga_{1-x}Mn_xAs$, LT-GaAs, and GaAs. Solid lines are linear fits for GaAs and $Ga_{0.97}Mn_{0.03}As$, respectively.

Figure 2 displays the temperature-dependent experimental results for $T_p(\lambda=800$ nm), and the corresponding C_{11}. Our measured results for GaAs agree quite well with previously reported values.[17,18] It can also be seen that GaAs and LT-GaAs have very similar C_{11} in the studied temperature regime. This indicates that the disordering effect caused by the large number of As_{Ga} antisite defects (with a concentration ~10^{19} cm^{-3}) in LT-GaAs plays a minor role in the mechanical properties along [001]. Figure 2 demonstrates that C_{11} measured for the $Ga_{1-x}Mn_xAs$ ($x=0.03$, 0.05, and 0.07) samples are also close to each other and hence have similar mechanical properties. Surprisingly, we found that C_{11} increase with T ($\delta C_{11}/\delta T>0$) in the $Ga_{1-x}Mn_xAs$ samples, in striking contrast to their behavior in both GaAs and LT-GaAs, where they are observed to decrease as the temperature increases ($\delta C_{11}/\delta T<0$). A linear fitting of C_{11} was carried out for GaAs and $Ga_{0.97}Mn_{0.03}As$, respectively. The fitting yields $C_{11}(\text{GaAs})=121.2-6.09\times10^{-3}$ T (GPa) and $C_{11}(Ga_{0.97}Mn_{0.03}As)=113.3+8.68\times10^{-3}$ T (GPa). It can also be seen that the obtained C_{11} for the ferromagnetic $Ga_{1-x}Mn_xAs$ system are systematically smaller than for GaAs or LT-GaAs in the studied temperature range. Specifically, the relative change $|C_{11(\text{GaAs})}-C_{11(\text{GaMnAs})}|/C_{11(\text{GaMnAs})}$ increases from ~3% at 295 K to ~6% at 78 K. In fact, V_s shows a similar behavior as that of C_{11}.

TABLE I. Calculated elastic constants of bulk GaAs, zinc-blende bulk MnAs, and $Ga_{1-x}Mn_xAs$ ($x=0.03$).

	GaAs	MnAs (zinc blende)	$Ga_{1-x}Mn_xAs$ ($x=0.03$)
C_{11} (GPa)	102.2	62.0	93.4
C_{12} (GPa)	41.4	59.1	45.1
C_{44} (GPa)	56.0	2.2	47.6
$B=(C_{11}+2C_{12})/3$ (GPa)	61.7	60.2	61.22

IV. DISCUSSION

To understand the decrease of C_{11} in $Ga_{1-x}Mn_xAs$, we performed spin-polarized density-functional calculations of the elastic constants for $x=0.03$ within the generalized gradient approximation using the VASP code.[21] Ultrasoft pseudopotentials for Ga, Mn, and As were employed. The plane-wave cut-off energy was set to 450 eV. For the elastic constants C_{11} and C_{12}, we follow the method proposed by Nielsen and Martin[22] while C_{44} is obtained according to Mehl *et al.*[23] The calculated results are listed in Table I. Despite the absolute deviation from the experimental values, the C_{11} (93.4 GPa) of $Ga_{1-x}Mn_xAs$ is found to decrease by 8.6 % at 0 K compared to that (102.2 GPa) of GaAs, consistent with the experimental observation (decrease by ~3% at 295 K and ~6% at 78 K). In Figs. 3(a) and 3(b), we further show the charge-density difference for the strained and unstrained bulk GaAs and $Ga_{1-x}Mn_xAs$, respectively. The charge densities of uniaxially strained crystals reveal interesting information on how electrons as well as nuclear positions respond to macroscopic strain. A small strain $\varepsilon_1=-0.01$ is applied along [100] in GaAs and $Ga_{1-x}Mn_xAs$, respectively. As shown in Fig. 3(b), the substitutional Mn_{Ga} doping induces an evident charge accumulation near the Mn nuclei, indicating that Mn-As bond becomes more ionic. Moreover, the effect of Mn doping is rather long-range: charge distributions are significantly distorted up to the third neighbors compared to GaAs.

The above calculations combined with the phenomenological Keating model[24] may give a more understandable picture. According to Keating,[24] $C_{11}=\alpha(1+3\beta/\alpha)/4a_0$, where α is the central (or bond-stretching) force constant, β is the mean value of the noncentral (or bending) force constant, and a_0 is the lattice constant. Since the lattice constant varies only slightly with substitutional Mn_{Ga} doping, the contribution from a_0 of the as-grown $Ga_{1-x}Mn_xAs$ ($0.03 \leq x \leq 0.07$) is expected to be negligible (<0.4%). On the other hand, the ionicity of a material can be characterized by the ratio β/α.[25] Ideally, the stronger the ionicity, the smaller the quantity β/α.[25] Therefore, β/α in the presence of Mn is expected to decrease compared to GaAs. This illustrates why the elastic constants in $Ga_{1-x}Mn_xAs$ become smaller than those in GaAs.

The temperature dependence of the elastic constant C_{11} in GaAs is in accord with the theoretical expectation. Namely, from 78 to 295 K, the elastic constant C_{11} almost decreases linearly with increasing temperature.[26,27] In contrast, C_{11} of $Ga_{1-x}Mn_xAs$ shows peculiar temperature behavior, i.e., it increases with increasing T, as shown in Fig. 2(b). Apparently, upon doping by a small fraction of Mn, the elastic properties of GaAs are altered dramatically. Although the underlying mechanism is not fully understood at present, it might be similar to the mechanism for phenomena observed in some transition metals: the shear elastic constants C_{44} of Nb, V, Ti, and some alloy systems were observed to show anomalous temperature behavior nearly thirty years ago.[28] The origin of this behavior has been ascribed to unique features of the Fermi surface in these systems.

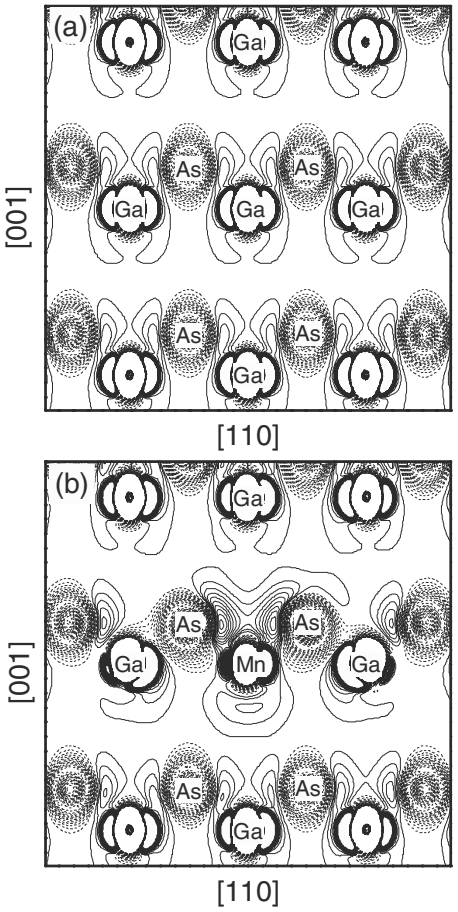

FIG. 3. Charge-density difference $\Delta\rho$ for (a) bulk GaAs and (b) $Ga_{1-x}Mn_xAs$ ($x=0.03$) in the {110} plane which contains a zigzag atomic chain. $\Delta\rho$ is defined as the charge density of a strained crystal minus the charge density of an unstrained crystal. The applied strain is $\varepsilon_1=-0.01$. Contour steps are 4×10^{-4} e/Å^3 and solid (dashed) contours indicate charge accumulation (depletion).

In our experiments, since $T_p \propto 1/n$ and $\tau \propto 1/k$, systematic analysis of T_p and τ as function of wavelength promises to provide some important insights into the electronic structure of the $Ga_{1-x}Mn_xAs$ system. Figures 4 and 5 show our experimental oscillation period T_p and decay time τ as a function of probe wavelength λ for $Ga_{1-x}Mn_xAs$, LT-GaAs, and GaAs measured at 78 K. As can be seen from Fig. 4, the oscillation periods are close to linear as a function of probe light wavelength for GaAs. This behavior agrees with the expression $T_p=\lambda/(2nV_s)$. In addition, the profile of $T_p(\lambda)$ for LT-GaAs is very similar to that for GaAs. This indicates that both mechanical and optical properties of these two materials are

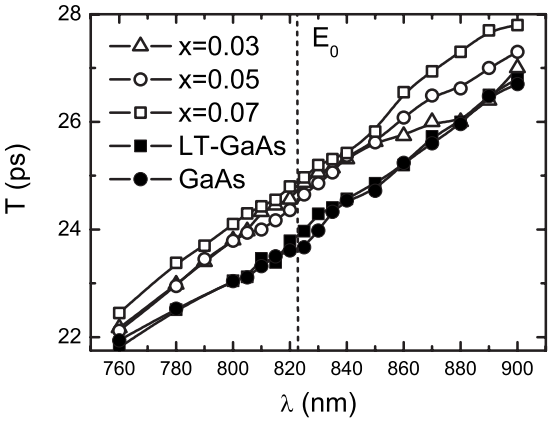

FIG. 4. Oscillation period T_p as a function of the wavelength λ of probe light for $Ga_{1-x}Mn_xAs$, LT-GaAs, and GaAs at 78 K. Dashed line represents the position of the critical point E_0 of GaAs.

close or that the As antisite defects play no strong role in determining V_s and n. However, the $T_p(\lambda)$ curves for $Ga_{1-x}Mn_xAs$ $(0.03 \leq x \leq 0.07)$ differ greatly from those for GaAs or LT-GaAs. This implies that there is a big difference in V_s and n between $Ga_{1-x}Mn_xAs$ and GaAs or LT-GaAs. Such differences have already been confirmed in our discussion above as well as by previous optical measurements.[3,10] Also, in the $Ga_{1-x}Mn_xAs$ samples we find that the $T_p(\lambda)$ curve begins to strongly deviate from linear dependence in the long wavelength regime (>850 nm). This observation has to be associated with a distinct nonlinear $n(\lambda)$ dependence for wavelengths corresponding to energies below the GaAs fundamental band gap E_0. The disordering effects are known to change optical properties (e.g., n and κ) in the material.[3,10] Therefore, comparison of T_p in $Ga_{1-x}Mn_xAs$ and LT-GaAs indicates that such strong nonlinearity is mainly due to Mn impurities rather than the As antisite defects.

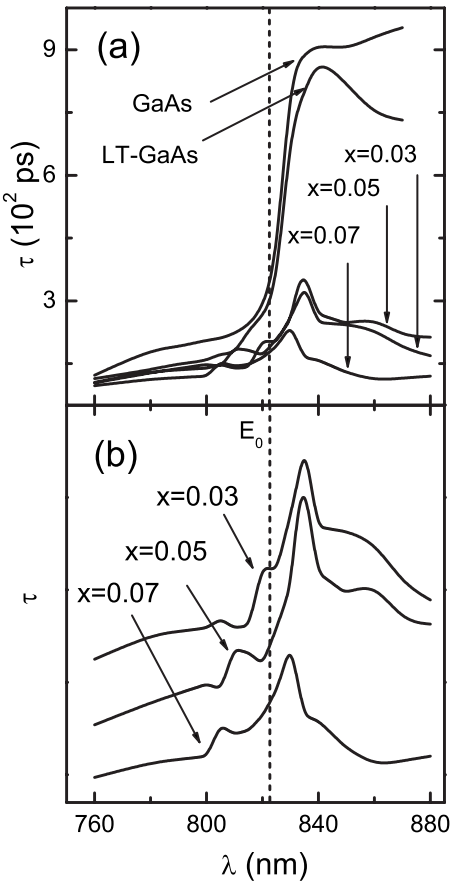

FIG. 5. (a) Damping time τ as a function of the wavelength λ of probe light for $Ga_{1-x}Mn_xAs$, LT-GaAs, and GaAs at 78 K. Dashed line represents the position of the critical point E_0 of GaAs. In (b), curves for $Ga_{1-x}Mn_xAs$ are shifted downward with increasing x to more clearly show the blueshift.

In Fig. 5(a), a sharp change in GaAs profile can be seen around 1.51 eV (~821 nm indicated by the dash line), which is the fundamental band gap (the critical point E_0 in energy). This kind of feature becomes diminished in LT-GaAs and disappears in the $Ga_{1-x}Mn_xAs$ systems. It is consistent with previous studies on $Ga_{1-x}Mn_xAs$,[3,10] where the band gap is broadened due to the As_{Ga} antisites and Mn impurities.

A closer look at the details of the damping time $\tau(\lambda)$ in Fig. 5(b), reveals the following important features. The structure of $\tau(\lambda)$ gradually evolves from a sharp steplike feature near E_0 in the GaAs data into a multipeak structure in $Ga_{1-x}Mn_xAs$. Surprisingly, the multipeak structure clearly blueshifts with Mn doping. This finding may imply a blueshifting of the fundamental band gap as Mn concentration increases. Such shifting has never been directly observed before although magnetic circular dichroism experiments suggest that E_0 blueshifts slightly with doping.[29] First, the compressive strain in the $Ga_{1-x}Mn_xAs$ film cannot account for such blueshift.[10] In order to fully understand this observation, one needs to examine the electronic structure of ferromagnetic $Ga_{1-x}Mn_xAs$. It should be pointed out that there are two scenarios proposed to describe this system: the debate is whether the Fermi energy sits inside the GaAs heavy and light hole VB or inside an Mn-induced IB above the top of GaAs VB.[3] However, we cannot attribute the observed blueshift to the VB scenario since Zhang and Sarma theoretically predicted on the basis of the VB scenario that as x increases the band gap becomes smaller resulting in a redshifting in the $Ga_{1-x}Mn_xAs$ system.[30] Thus, our results indicate that the VB scenario does not adequately describe the Mn-doped GaAs band structure. Thus, we conclude that the blueshifting should be associated with the Mn-induced IB. As is known, a p-d hybridization exists between the Mn-induced IB and the GaAs VB. Such hybridization is k dependent and very strong near the L point, which explains the observed large blueshift of the critical point E_1 in Ref. 10. Therefore, although the k-dependent p-d hybridization is expected to be small around the Γ point, our experiments indicate that the small V_{pd} still can lead to the observable blueshifting around the fundamental band gap as long as the experimental technique is sensitive enough to reveal this subtle feature.

V. CONCLUSIONS

In conclusion, employing femtosecond two-color pump-

-probe spectroscopy we have carried out an analysis of the pronounced oscillatory behavior observed in the reflectivity curves of magnetic semiconductor GaMnAs systems. We report experimental values of the elastic constant C_{11} in ferromagnetic $Ga_{1-x}Mn_xAs$ samples. Both V_s and C_{11} in the GaMnAs systems are found to be systematically smaller than in GaAs at temperature between 78 and 295 K. The temperature dependence of C_{11} for $Ga_{1-x}Mn_xAs$ and GaAs shows totally different behavior. The slight but marked blueshifting associated with the fundamental band gap as Mn doping increases in $Ga_{1-x}Mn_xAs$ system was directly observed and is attributed to the hybridization of the Mn IB with the GaAs VB.

ACKNOWLEDGMENTS

This work was supported at Vanderbilt by DOE under Grant No. DE-FGO2–99ER45781 and at Notre Dame by NSF under Grant No. DMR06–03762. J. Yan and S. T. Pantelides acknowledge the McMinn Endowment at Vanderbilt University.

[1] H. Ohno, Science **281**, 951 (1998).
[2] J. Jungwirth, J. Sinova, J. Masek, J. Kucera, and A. H. MacDonald, Rev. Mod. Phys. **78**, 809 (2006) and references therein.
[3] K. S. Burch, D. D. Awschalom, and D. N. Basov, J. Magn. Magn. Mater. **320**, 3207 (2008).
[4] *Semiconductor Spintronics and Quantum Computation*, edited by D. D. Awschalom, N. Samarth, and D. Loss (Springer, New York, 2002).
[5] U. Welp, V. K. Vlasko-Vlasov, X. Liu, J. K. Furdyna, and T. Wojtowicz, Phys. Rev. Lett. **90**, 167206 (2003).
[6] M. Sawicki, F. Matsukura, A. Idziaszek, T. Dietl, G. M. Schott, C. Ruester, C. Gould, G. Karczewski, G. Schmidt, and L. W. Molenkamp, Phys. Rev. B **70**, 245325 (2004).
[7] T. Dietl, H. Ohno, and F. Matsukura, Phys. Rev. B **63**, 195205 (2001).
[8] M. Abolfath, T. Jungwirth, J. Brum, and A. H. MacDonald, Phys. Rev. B **63**, 054418 (2001).
[9] A. M. Yakunin, A. Yu. Silov, P. M. Koenraad, J.-M. Tang, M. E. Flatté, J.-L. Primus, W. Van Roy, J. De Boeck, A. M. Monakhov, K. S. Romanov, I. E. Panaiotti, and N. S. Averkiev, Nature Mater. **6**, 512 (2007).
[10] K. S. Burch, J. Stephens, R. K. Kawakami, D. D. Awschalom, and D. N. Basov, Phys. Rev. B **70**, 205208 (2004).
[11] C. Thomsen, H. T. Grahn, H. J. Maris, and J. Tauc, Phys. Rev. B **34**, 4129 (1986).
[12] O. B. Wright, J. Appl. Phys. **71**, 1617 (1992).
[13] H.-Y. Hao and H. J. Maris, Phys. Rev. Lett. **84**, 5556 (2000).
[14] S. Wu, P. Geiser, J. Jun, J. Karpinski, and R. Sobolewski, Phys. Rev. B **76**, 085210 (2007).
[15] J. K. Miller, J. Qi, Y. Xu, Y.-J. Cho, X. Liu, J. K. Furdyna, I. Perakis, T. V. Shahbazyan, and N. Tolk, Phys. Rev. B **74**, 113313 (2006).
[16] A. Devos, F. Poinsotte, J. Groenen, O. Dehaese, N. Bertru, and A. Ponchet, Phys. Rev. Lett. **98**, 207402 (2007).
[17] Yu. A. Burenkov, Yu. M. Burdukov, S. Yu. Davidov, and S. P. Nikanorov, Sov. Phys. Solid State **15**, 1175 (1973).
[18] J. S. Blakemore, J. Appl. Phys. **53**, R123 (1982); M. R. Brozel and G. E. Stillman, *Properties of Gallium Arsenide*, 3rd ed. (Institute of Engineering and Technology, Knovel Corporation, 1996).
[19] E. J. Singley, K. S. Burch, R. Kawakami, J. Stephens, D. D. Awschalom, and D. N. Basov, Phys. Rev. B **68**, 165204 (2003).
[20] A. Steigerwald, Y. Xu, J. Qi, J. Gregory, X. Liu, J. K. Furdyna, K. Varga, A. B. Hmelo, G. Lüpke, L. C. Feldman, and N. Tolk, Appl. Phys. Lett. **94**, 111910 (2009).
[21] G. Kresse and J. Furthmüller, Phys. Rev. B **54**, 11169 (1996).
[22] O. H. Nielsen and R. M. Martin, Phys. Rev. B **32**, 3792 (1985).
[23] M. J. Mehl, B. M. Klein, and D. A. Papaconstantopoulos, in *Intermetallic Compounds: Principles and Practice*, edited by J. H. Westbrook and R. L. Fleischer (Wiley, New York, 1995), Vol. I, Chap. 9, pp. 195–210.
[24] P. N. Keating, Phys. Rev. **145**, 637 (1966).
[25] R. M. Martin, Phys. Rev. B **1**, 4005 (1970).
[26] M. Born and K. Huang, *Dynamical Theory of Crystal Lattice* (Oxford University Press, Oxford, 1954).
[27] Y. P. Varshni, Phys. Rev. B **2**, 3952 (1970).
[28] E. Walker and P. Bujard, Solid State Commun. **34**, 691 (1980) and references therein.
[29] K. Ando, H. Saito, K. C. Agarwal, M. C. Debnath, and V. Zayets, Phys. Rev. Lett. **100**, 067204 (2008).
[30] Y. Zhang and S. Das Sarma, Phys. Rev. B **72**, 125303 (2005).